Pournasiri Poshtiri Maryam (Orcid ID: 0000-0002-2412-6092)

Variability Patterns of the Annual Frequency and Timing of Low Streamflow Days Across the USA and their linkage to regional and large-scale climate

Maryam Pournasiri Poshtiri[1,2], Indrani Pal[3,4], Upmanu Lall[3], Philippe Naveau[5], Erin Towler[6]

[1]Department of Civil Engineering, University of Colorado Denver, Campus Box 113, PO Box 173364, Colorado 80217-3364, US.

[2]Bryant Consultants, Inc., 3360 Wiley Post Road, Suite 100, Carrollton, Texas 75006, US.

[3]Columbia Water Center, The Earth Institute, Columbia University, New York City, New York, US

[4]NOAA Center for Earth System Sciences and Remote Sensing Technologies (NOAA-CREST), The City University of New York, New York City, New York, US

[5]Institut Pierre Simon Laplace, Laboratoire des Sciences du Climat et l'Environnement (LSCE) IPSL-CNRS, Gif-sur-Yvette FRANCE

[6] Mesoscale and Microscale Meteorology Laboratory, National Center for Atmospheric Research (NCAR), Boulder, Colorado, US

CORRESPONDING AUTORS:

Maryam Pournasiri Poshtiri[1,2]

Emails: maryam.pournasiriposhtiri@ucdenver.edu & mpournasiri@geoneering.com

Indrani Pal[3,4]

Emails: ipal@ccny.cuny.edu & ip2235@columbia.edu

ABSTRACT

Low flow events can cause significant impacts to river ecosystems and water-use sectors; as such it is important to understand their variability and drivers. In this study, we characterize the variability and timing of annual total frequency of low streamflow days across a range of headwater streams within the continental United States (US). To quantify this, we use a metric that counts the annual number of low flow days below a given threshold, defined as the Cumulative Dry days Occurrence (CDO). First, we identify three large clusters of streamgauge locations using a Partitioning Around Medoids (PAM) clustering algorithm. In terms of timing, results reveal that for most clusters, the majority of low streamflow days occur from the middle of summer until early fall, though several locations in Central and Western US also experience low flow days in cold seasons. Further, we aim to identify the regional climate and larger-scale drivers for these low streamflow days. Regionally, we find that precipitation deficits largely associate with low streamflow days in the western US, while within the central and eastern US clusters, high temperature indicators are also linked to low streamflow days. In terms of larger-scale, we examine sea surface temperature (SST) anomalies, finding that extreme dry years

2

exhibit a high degree of co-occurrence with different patterns of warmer SST anomalies across the Pacific and northern Atlantic Oceans. The linkages identified with regional climate and SSTs offer promise towards regional prediction of changing conditions of low streamflow events.

KEYWORDS: Cumulative Dry days Occurrence (CDO)**,** headwater streams, low streamflow, clusters, regional climate, larger-scale drivers

1 | INTRODUCTION

Every river or stream undergoes low flow events during the year (Smakhtin, 2001). The variability of low flow conditions (e.g. occurrence and magnitude) depend on several natural and human factors that impact the ecological flow regime (Van Loon, 2013). Most streams within the United States (US) experience annual variations of low flow conditions as a function of rainfall, snowmelt, catchment characteristics, land-use/land-cover, water control infrastructures, water withdrawals, and water discharges, etc. Low flows matter for maintaining water quality and can be used to set pollution discharge permit limits. Within US streams, the design flow statistic that is often used to define low flow conditions is the minimum 7-day mean flow that occurs on average once every 10 years (10q7) (US EPA, 2017). Once this limit is crossed, the stream is considered to be in a low flow event. Many water-using sectors care about low flow events, such as agriculture, navigation, recreation, and hydropower; these sectors are interested in information

3

on when in a year low flows can occur in a river/stream (e.g. occurrence timing), or how frequently/long low flow days can occur/persist within a specific time period and location of interest (e.g. cumulative occurrence in a year or season), or how far below a threshold can a streamflow (e.g. below 10q7 threshold) (Kroll & Vogel, 2000; Kroll et al., 2004). A variety of ecological outcomes depend on low flow conditions. One example, in the US context, is federally endangered fish species, such as chinook and coho salmon, and steelhead trout productivity in coastal California and Pacific Northwest, where spawning and migration patterns of these species depend largely on low flow and associated hydrological conditions (Waples et al., 2008).

Most natural streams within the US experience annual variation of low flow events (Pournasiri Poshtiri et al., 2018). Observed natural low flow records indicated a gradual drying tendency of headwater locations in several major river basins of the US (Pournasiri Poshtiri & Pal, 2016). Under changing climatic conditions and land use modifications, more and more headwater perennial streams are expected to turn intermittent (Datry et al., 2016; Döll & Schmied, 2012; Jaeger et al., 2014; Reynolds et al., 2015), often with longer-term implications on local biodiversity and ecosystem functions (Bogan et al., 2015; Datry et al., 2016; Leigh & Datry, 2017; Najafi et al., 2018; Vander Vorste et al., 2016; Wohl, 2017). These changes do not seem to be happening at one specific location in isolation, rather, they have been found to be happening at the same time in a cluster of adjacent sites (Pournasiri Poshtiri & Pal, 2016), which could be associated with regional climatic conditions and human disturbances. Recent studies

4

indicate that naturally occurring and or managed streamflow stations within the US show similar responses to changes within the major river basins (Ficklin et al., 2018), indicating that water management and land-cover changes have not substantially altered the effects of climate on human-modified watersheds, as compared to the neighboring natural streams. Further, variations in streamflow over different parts of the US, and their regional climate drivers (e.g. temperature, precipitation) have been reported to be tele-connected to larger-scale ocean-atmospheric patterns in the Pacific or Atlantic Oceans (Armal et al., 2018; Baek et al., 2017; Berton et al., 2017; Cook et al., 2011; Feng et al., 2011; Ho et al., 2018; Ladd et al., 2018; Najafi et al., 2019; McCabe et al., 2008; Oglesby et al., 2012). Therefore, it is of interest to identify clusters of stream gage locations where annual variation of low flow incidence characteristics are of similar nature, and to investigate their association with climate variability, at both regional and larger-scales.

In the US, there are relatively few recent studies that have deeply investigated the variability of low flow incidence frequency and their climatic associations. Reynolds et al. (2015) found an increase in the frequency of zero-flow days in the upper Colorado River basin in the dry precipitation years, associated with high temperatures and low precipitation (Reynolds et al., 2015). Eng et al. (2016) identified five distinct seasonality patterns in the zero-flow events in the US and strong correlation patterns with historical variations in climate. Sadri et al. (2016) reported that many stream gauge locations in the eastern US experiencing low flow events in late summer to fall, driven by the precipitation deficit and high evaporative demand. Berton et al. (2017) reported a strong teleconnection between the historic occurrence of the relative frequency

5

of dry streamflows but for the northeastern US alone – connecting with the extreme phases of Atlantic Multi-decadal Oscillation (AMO) and the North Atlantic Oscillation (PDO). Dierauer et al. (2018) classified low flow regimes and separated summer versus winter low flows in snow-covered catchments in western US. They found that the co-occurrence of warm and dry winter conditions leads to significantly longer, more severe summer low flow events and shorter winter low flow events (Dierauer et al., 2018). Recently, a study by Pournasiri Poshtiri et al. (2018) compared the spatial variability of low flow magnitude indicators versus defiict indictors, showing that magnitude indicators are significatly different from the deficit indicators, though they show similar linkages to the regional climate and meteorological drought (Pournasiri Poshtiri et al., 2018).

Building on the previous studies, the purpose of this study is to characterize the variability of annual total frequency of low streamflow days and their potential climate drivers. First, we calculate the frequency of low streamflow days, defined as the Cumulative Dry days Occurrence (CDO), across a range of headwater streams within the US. Next, we apply a non-parametric data driven clustering algorithm to identify the spatial patterns of the annual CDO. Then, we calculate the occurrence timing of CDO. Further, we aim to identify the regional climate and larger-scale drivers for these low flow events. To this end, we examine the relationships between the CDO variability within each cluster and regional and larger-scale climate drivers.

6

We organize this paper as follows: section 2 describes the data used in this study and section 3 presents the detailed assessment methods. Section 4 presents results, and section 5 presents the summary and discuss the outcomes.

2 | DATA

2.1 | Annual Cumulative Low Streamflow Days Occurrence (CDO)

We calculate CDO using daily streamflow records from the U.S. Geological Survey Hydro-Climatic Data Network 2009 (HCDN-2009). There are 603 streamflow stations with between 25 (1987-2012) to 111 years (1901-2012) of daily data and we only consider stations with less than 10 percent missing values. Geographic locations of the stations are presented in Figure 1. HCDN-2009 represents headwater type stations whose flows are minimally impacted by human development (Lins, 2012). This data network is a valuable indication of observed natural streamflow records and has been employed in many streamflow studies (Frei et al., 2015; Kam & Sheffield, 2016; Newman et al., 2015; Pournasiri Poshtiri & Pal, 2014; Pournasiri Poshtiri & Pal, 2016; Pournasiri Poshtiri et al., 2018; Rossi et al., 2016; Timilsena et al., 2009; Vidal et al., 2010). We define the climate year to be from April to March for all the analyses; this is so streamflow from the entire dry season are included in the annual values (Cravotta, 1982; Martin & Arihood, 2010; Martin et al., 2016; US EPA, 2017).

CDO is calculated using the threshold level method (Yevjevich, 1967), where the total number of days with flows going under a specific threshold are counted per year. Threshold

7

methods are the most frequently applied quantitative method to identify deficit characteristics from time series variables (Pournasiri Poshtiri et al., 2017; Tallaksen et al., 1997; Van Loon, 2013). To calculate the threshold level, we first calculate the annual minimum 7-day mean river flow magnitude from the daily time series streamflow in each station (q7, low flow), and then, we determine the 10-year return value of q7 over the entire annual time series in each station (10q7). Under the stationary assumption, 10q7 is the lowest 7-day average flow that occurs once every 10 years. After that, we calculate CDO as the total number of days falling below 10q7 within each climate year. The CDO 10q7 indicator dataset used in this analysis is freely available for download from NCAR's research data archive (https://rda.ucar.edu/datasets/ds550.0/) (Pournasiri Poshtiri et al., 2016).

2.2 | Regional climate indicators

To explore associations between the CDO and regional climate, we calculate several regional climate indicators using daily temperature and precipitation data from the United States Historical Climatology Network (USHCN) (Menne et al., 2010). The USHCN stations represent long term high quality daily data from 1218 observing stations across the US (Menne et al., 2010). Using this dataset, we calculate cumulative precipitation dry days as total annual number of days with precipitation less than 1 mm (P_{cpd}). In addition, we compute four temperature indicators including annual maximum value of daily maximum temperatures (T_{max}), annual 95th

8

percentile value of daily maximum temperatures (T_{95}), annual mean value of diurnal temperature ranges (T_{dtr}), and annual mean daily temperature (T_{ave}).

We further check associations between annual meteorological drought indicator and CDO. We use the Palmer Modified Drought Index (PMDI) as meteorological drought indicator. This is a one-degree gridded monthly data product developed for the continental US, covering the period of 1895 to 2004. PMDI is a measure of meteorological drought/floods accounting for evapotranspiration, soil moisture and precipitation conditions in a region (Heim et al., 2007).

2.3 | Larger-scale climate drivers

For the larger-scale climate drivers, we investigate SST anomalies. We select Extended Reconstructed SST anomalies from NOAA NCDC ERSST version3b, obtained in ready-to-analyze format from the IRI Data Library (http://iridl.ldeo.columbia.edu). This version of ERSST is optimally tuned to exclude under-sampled regions for global averages and it does not involve satellite data, which may cause a cold bias significant enough to change the rankings of months (Smith et al., 2008).

3 | METHODS

3.1 | Spatial clustering of CDO

We use the Partitioning Around Medoids (PAM) algorithm based on the F-madogram (Bernard et al., 2013) to identify regions with similar CDO variability. The PAM algorithm

9

generates clusters around representative stations called medoids. A medoid is a station where the CDO time series best represents the statistical distribution of the data within the other stations in the cluster (Bernard et al., 2013; Kaufman & Rousseeuw, 2009). The F-Madogram measures the pairwise dependence among CDO time series in each cluster and it is used as distance metric in the PAM algorithm (Bernard et al., 2013). The F-Madogram is defined as:

$$d_{ij} = \frac{1}{2T} \sum_{t=1}^{T} |\widehat{F}_i(M_i^{(t)}) - \widehat{F}_j(M_j^{(t)})| \tag{1}$$

where $(M_i^{(t)}, M_j^{(t)})^T$ are CDO time series from two locations i and j at T different time units and $\widehat{F}_i$ is the empirical distribution function, expressed as (van der Vaart, 1998):

$$\widehat{F}_i(u) = \frac{number\ of\ elements\ in\ the\ sample \leq u}{T} \tag{2}$$

Thus, to run the PAM algorithm, the distance metric d_{ij} needs to be computed using equation 1 and the number of clusters K has to be specified. For a given K, the PAM algorithm divides a CDO data points into K clusters and assigns the random different medoids (Bernard et al., 2013). Then, PAM algorithm moves around K medoids and tries to minimize total intra-cluster distance (Bernard et al., 2013). At each step of the algorithm, a medoid represents one station of a valid CDO time series. Consequently, we determine the optimal number of clusters and significance level of silhouette coefficient as follows:

To choose the optimal number of clusters, K, we use silhouette coefficients (SC) (Zelenhasić & Salvai, 1987). SC provides a fair comparison between the cohesion and separation of K clusters (Bernard et al., 2013; Bracken et al., 2015; Najafi et al.,2018). By considering d_{iK}

10

as the F-Madogram distance between a station i and its own cluster medoid and $d_{i,-K}$ as the smallest F-Madogram distance between the same station i and all the other medoids, the silhouette coefficient ($SC_i(K)$) for a station i is defined as:

$$SC_i(K) = 1 - \frac{d_{iK}}{d_{i,-K}} \tag{3}$$

A positive $SC_i(K)$ indicates that the intracluster distance is smaller than the intercluster distance and station i is well-classified; a negative or zero $SC_i(K)$ indicates that station i is either non-informative or non-classified (Bernard et al., 2013).

We run the PAM algorithm for a given number of K values and calculate SC each time for each station i. Then, we use the average of all SC for the evaluation of the number of clusters and determine the optimal number of clusters (e.g., Bernard et al., 2013; Pournasiri Poshtiri et al., 2018).

We further determine if a $SC_i(K)$, as calculated above is statistically significant. We determine 95th percentile levels of SCs for each given K under a null hypothesis that there is no clustering structure in the CDO dataset. To do that we shuffle the CDO dataset at each station along each time series, sample that randomly, and run the PAM algorithm on this time series. This randomization removes spatial and temporal dependency (Bernard et al., 2013). We repeat this algorithm 50 times, and then select the 95% quantile value from 50 average SCs as the statistical significance level. The initial SC values falling below the 95th percentile threshold could just happen due to chance. Hence, stations corresponding to the SCs falling below this threshold are not well classified, which are not considered for further analyses.

11

We conduct the clustering analysis for using several different data length criteria, including (1) 557 stations with 30 years of data from 1983 to 2012, (2) 466 stations with 40 years data from 1873 to 2012, and (3) 393 stations with 50 years data from 1963 till 2012. The results are presented in section 4.1.

3.2 | Occurrence timing of CDO

To understand when in the year low flow days are most likely to occur in each cluster, we explore the timing of the CDO. First, we determine the average number of days falling below 10q7 within each month for each station. Then, for each cluster, we can calculate the percentage of stations that experience on average the number of days below 10q7 in each month. The result is shown in section 4.2.

3.3 | Connections between CDO and climate

Finally, we examine the relationships between the regional and larger-scale climate indicators (specified in sections 2.2 and 2.3) and CDO. Due to the high spatial variability in the time series of CDO within each cluster, we consider a combined version of all the CDO time series within each cluster—the combined cumulative streamflow dry days (CCDO), as follows:

$$\text{CCDO} = \frac{\sum_{i=1}^{n}(\text{CDO\_Z}_i * \text{SC}_i)}{\sum_{i=1}^{n}\text{SC}_i} \tag{4}$$

Where CDO_Z_i is the transformed CDO data on the z-scale at each station i that has a significant SC value i.e. value higher than the 95th quantile threshold. CCDO for each cluster

12

represents variability of annual drying frequency of rivers within the same cluster and is further used to investigate regional and larger-scale climate connections.

We use the non-parametric Kendall rank correlation test to determine if the regional climate variables are significantly correlated at the 5% significance level with each cluster's CCDO. We also use composite analysis to further explore the regional and large scale climate connection with CCDO.

4 | RESULTS

4.1 | Clustering patterns of CDO with similar variability

Here, we present the detailed analysis for 50-years of CDO data (1963-2012) for 393 stations because this data length provides a good tradeoff between the number of years used in the study and corresponding number of stations, providing a fair spatial distribution for clustering analysis (referred to section S1 in Supplementary Information). Figure 2a shows the distribution of silhouette coefficients for the 50 years CDO data. The red line represents average SC values for each given K, and the dotted blue line displays 95th percentile values of SCs (method discussed in section 3.1). We select the K based on the highest average SC value as well as lower number of stations having negative SC values (i.e. non-classified stations). Figure 2b displays spatial pattern for K=3 where three corresponding medoid stations are indicated by triangles and the non-classified stations are displayed as grey circles. K=3 divides the US into three large regions (the east, central, and the west) where CDO varies distinctively and the

13

medoids do not show any significant correlations (Figure s4a in section S3). This indicates that the clustering algorithm was able to identify three distinct variability patterns in CDO. Unlike that, the second best K=12 (Figure 2a) creates smaller clusters throughout the US (Figure s3c), where medoids in the nearby clusters display correlations (detailed analysis in section S2 and S3).

CDO for each distinct cluster in Figure 2b indicates spatial variability in themselves (section S3 and Figure s5). Therefore, as indicated in the methods section, we combine the data by only incorporating stations that are statistically significant, to develop CCDO (equation 4). CCDO captures regional fluctuation of the data well (Figure s7), which we use further to investigate the relationships between frequency of low flow days within each cluster and climate indicators.

4.2 | Occurrence timing of CDO

Our analysis shows that the majority of the stations within each cluster experience the highest frequency of low flow days within the middle of summer to early fall (Figure 3). In the eastern US (cluster 1 in Figure 3aa), 94.8% of the stream gauge stations experience low flow days from August to October (i.e., 24.3% in August, 53.9% in September, 14.2% in October). In the central US (Cluster 2 in Figure 3ba), 63.3% of the stations experience low flow days between August and October (i.e., 30.3% in August, 21.2% in September, and 12.1% in October), while a significant proportion of the stations also experience low flows during April (25.3%). In the

14

western US (Cluster 3, Figure 3ca), nearly 80.6% stations experience low flows during August-October (i.e., 13% in August, 54.6% in September, and 14.2% in October), with some stations experiencing in February (5.2%), March (2.6%), and April (7.8%) as well.

4.3 | Climate connectivity with CDO

4.3.1 | Regional climate connectivity

Table 1 represents the percent of climate stations with statistically significant correlation at the 5% significance level with the CCDO of each cluster and Figure 4 shows the spatial plots for each of the regional climate variables. In general, more than 80% of the grid cells (bolded cells in Table 1) display the significant correlation between PMDI and CCDO across all clusters (Figure 4a), indicating that PMDI has the strongest relationship with the CCDO for every region of the US. Strong negative associations between the CCDO and PMDI within corresponding clusters indicate the high sensitivity of cumulative frequency of low flow days to regional evapotranspiration, soil moisture conditions, and precipitation (i.e., the variables that contribute to the PMDI calculation). However, to further understand which of the variables underlying the PMDI are the most influential, we also examine the CCDO correlations with regional precipitation and temperature indicators. For all the clusters, a high percentage of P_{cpd} stations (more than 50%, bolded in Table 1) display significant correlations with CCDO (Figure 4b). In the western US (Cluster 3), in addition to P_{cpd}, T_{avg} also plays a significant role (Table 1). On the other hand, when we move from western parts (Cluster 3) to the eastern parts of the US (Cluster

15

1 and 2 in Table 1 and Figure 4), the high temperature indicators (i.e., T_{max}, T_{95}, T_{dtr}) display significant correlations, while such a relationship is not seen in the western parts of the US. The temperature variable with the highest proportion of significant stations in the central US (Cluster 2) are T_{dtr} (65.45%, bolded in Table 1) and then T_{95} (51.95%, bolded in Table 1), and that in the eastern US (Cluster 1) are T95 (73.5%, bolded in Table 1) and T_{max} (69.13%, bolded in Table 1). For the sake of completeness, we repeated the above analyses for K=12 and we observed the similar relationships in the eastern, central, and western clusters (Section S5 and Figure s11).

The above findings are further substantiated when we explore the anomalies of the climate indicators over the driest CCDO years. To this end, we first extracted the extreme dry years (years when CCDO values fell above long-term 75th percentile threshold, shown in Figure s9). As a result, the driest years within each cluster co-occurred with known meteorological dry years (e.g., 1988, 2002), as well as persistent dry years (e.g., 1991-1995, 1999–2004, 2011-2012). For a more detailed discussion on the correspondence between CCDO and meteorological droughts in the history of US, please refer to the supplementary information (S5). We also look at the composite maps of different climate indicators over the driest years of CCDO for each cluster (Section S7, Figure s12). The results indicate that extremity of climate indicators and severely dry streamflow years co-occur with each other, mostly echoing the results within Figure 4.

4.3.2 | Larger-scale climate connectivity

16

Extreme hydrological events, including low flows, may correspond to atmospheric circulation anomalies forced by specific SST patterns in the oceans. Figure 5 shows three distinct patterns of SST anomalies in the Pacific and North Atlantic Oceans, corresponding to the driest years of CCDO. We conduct a significance testing of the composites by selecting any 15-year periods randomly at a time and determining the average SST anomaly values. SST anomaly composite magnitudes falling outside the 5th and 95th percentile ranges are considered significant. We find that the driest years in cluster 1 coincide with the warmer temperatures in the northwestern Pacific Ocean, leading to a tongue-like formation extending from the eastern coast of South Asia to the central north Pacific (PDO-like pattern), as well as with a warmer northern Atlantic Ocean between the southern coast of Greenland to Equator (Figure 5a). The driest years in cluster 2 correspond to a similar but weaker SST patterns corresponding to cluster 1, where SST in both oceans are predominantly warmer in the central northern Pacific area and along the coast of Greenland and other fragmented locations in the North Atlantic. Furthermore, extreme dry years occurring in cluster 3 co-occur with warmer SST anomaly in the northern as well as tropical Pacific Oceans, in addition to a warmer Northern Atlantic Ocean that is milder than the pattern corresponding to cluster 1. Overall, distinct SST anomaly and their combinations within the Pacific and Atlantic affect larger-scale wind and moisture flows differently into different regions of the US, affecting local precipitation and temperature variability, and in turn, influencing streamflow in different clusters of locations. Again, by repeating the same analysis

17

for K=12, we find that neighboring clusters display similar SST anomaly patterns (presented in section S8).

5 | SUMMARY AND DISCUSSION

In this study, we identified clusters of river headwater locations which are primarily driven by natural climate variability. Using a nonparametric data-driven clustering method, we identified distinct variability pattern in the frequency of low flow days in the US. There were three unique clusters, where low flow days mostly occurred in the summer and early fall months, which could be generated by climate extremes. The potential driving mechanisms were discussed in Pournasiri Poshtiri et al. (2018), where they concluded that in the western US, precipitation deficit seems to play the key role, leading in declining the soil moisture and generating low flows in summer-fall (Pournasiri Poshtiri et al., 2018). However, in the central and western regions, where the vegetation coverage is denser, increased evaporation during the warm season tend to drive low flows in summer and fall (Pournasiri Poshtiri et al., 2018). In this study, we also found some low flow days to occur in cold months specifically in snow-dominated regions in clusters 2 and 3. In those regions, cold seasons low flow days could be developed by two different mechanisms: First, low flow days in early cold seasons (November-December) could be processed by the summer-fall low flow days and warm/dry climate conditions. During sustained dry conditions, low streamflows are generally controlled by subsurface groundwater flows (Smakhtin, 2001; Van Loon, 2013), which may result in depletion of soil moisture storage and

18

the groundwater recharge (Dudley & Hodgkins, 2013) and consequently lead to low flow days occurrence in the early cold season. Second, in later months (February-April), low temperatures lead to snow and ice, causing zero or low flows from these cold-conditions, which consequently increase the occurrence of low flow days (Dierauer et al., 2018). Further, a high frequency of low flow events in late spring and early summer in the eastern cluster (Figure 3a) could be driven by human activities or groundwater depletion (Sadri et al., 2016), although we have tried to minimize these influences in this study by using headwaters gauges. We also conducted a comparative analysis between the CDO, a low flow occurrence indicator, and annual total number of days with zero flows, a river intermittency measurement, and found very similar results.

In this study, our aim was to capture the impacts of climate variability, at the regional and larger-scales, on the low flow events, such that we can identify the common climate indicators for low flow events within the cluster. However, we acknowledge that we do not investigate several other factors that could be important, such as catchment characteristics. Nevertheless, it is difficult to identify the most dominant processes on a catchment scale, especially underground processes that are difficult to observe. As such, several outstanding questions remain to be addressed, most importantly, what are the main catchment drivers of the frequency of the low flow in different seasons?

Further, we investigated the associations between SST anomalies and each cluster's driest years. This offers insights on the relative importance of SST teleconnections on extreme dry

19

phases of rivers. We highlight three significantly different patterns of SST anomaly in the Pacific and North Atlantic. Occurrence of warm SST anomaly in the northern Pacific and Atlantic Oceans could shift the atmospheric pressure patterns, and consequently, northerly wind anomalies reducing the flow of moist air into the continent and leading to reduced precipitation, and consequently result in high exceedances in the frequency of hot days over much of US (Donat et al., 2016).

Overall, this study provides a novel contribution on the characterizing of frequency and timing of low flow days across the US. We conclude that the occurrence of low flow days across the US are organized, occurring in clusters, where they significantly co-vary with regional climate variability as well as larger-scale SST patterns. Although other factors play an important role in low flow frequency and timing, such as groundwater interaction, catchment geology, and other human activities, this study did find significant associations with regional and larger-scale climatic drivers. This study suggests that region-specific climate indicators and SST anomalies can be used as potential predictors of frequency of low flow occurrence specific to each cluster, providing a context for the past and potential changes to streamflow nature in the US rivers.

REFERENCES

Armal, S., Devineni, N., & Khanbilvardi, R. (2018). Trends in extreme rainfall frequency in the contiguous united states: Attribution to climate change and climate variability modes. Journal of Climate, 31(1), 369-385.

20

Baek, S. H., Smerdon, J. E., Coats, S., Williams, A. P., Cook, B. I., Cook, E. R., & Seager, R. (2017). Precipitation, temperature, and teleconnection signals across the combined North American, Monsoon Asia, and Old World Drought Atlases. *Journal of Climate*, *30*(18), 7141–7155.

Bernard, E., Naveau, P., Vrac, M., & Mestre, O. (2013). Clustering of maxima: Spatial dependencies among heavy rainfall in France. *Journal of Climate*, *26*(20), 7929–7937.

Berton, R., Driscoll, C. T., & Adamowski, J. F. (2017). The near-term prediction of drought and flooding conditions in the northeastern United States based on extreme phases of AMO and NAO. *Journal of Hydrology*, *553*, 130–141.

Bogan, M. T., Boersma, K. S., & Lytle, D. A. (2015). Resistance and resilience of invertebrate communities to seasonal and supraseasonal drought in arid   ‐land headwater stream *Freshwater Biology*, *60*(12), 2547–2558.

Bracken, C., Rajagopalan, B., Alexander, M., & Gangopadhyay, S. (2015). Spatial variability of seasonal extreme precipitation in the western United States. *Journal of Geophysical Research: Atmospheres*, *120*(10), 4522–4533.

Cook, B. I., Seager, R., & Miller, R. L. (2011). Atmospheric circulation anomalies during two persistent North American droughts: 1932–1939 and 1948–1957. *Climate Dynamics*, *36*(11–12), 2339–2355.

Cravotta, C. A. (1982). *US geological survey water-supply paper*. US Government Printing Office.

21

Datry, T., Fritz, K., & Leigh, C. (2016). Challenges, developments and perspectives in intermittent river ecology. *Freshwater Biology*, *61*(8), 1171–1180.

Dierauer, J. R., Whitfield, P. H., & Allen, D. M. (2018). Climate Controls on Runoff and Low Flows in Mountain Catchments of Western North America. *Water Resources Research*.

Döll, P., & Schmied, H. M. (2012). How is the impact of climate change on river flow regimes related to the impact on mean annual runoff? A global-scale analysis. *Environmental Research Letters*, *7*(1), 14037.

Donat, M. G., King, A. D., Overpeck, J. T., Alexander, L. V, Durre, I., & Karoly, D. J. (2016). Extraordinary heat during the 1930s US Dust Bowl and associated large-scale conditions. *Climate Dynamics*, *46*(1–2), 413–426.

Dudley, R. W., & Hodgkins, G. A. (2013). Historical groundwater trends in northern New England and relations with streamflow and climatic variables. *JAWRA Journal of the American Water Resources Association*, *49*(5), 1198–1212.

Eng, K., Wolock, D. M., & Dettinger, M. D. (2016). Sensitivity of intermittent streams to climate variations in the USA. *River Research and Applications*, *32*(5), 885–895.

Feng, S., Hu, Q., & Oglesby, R. J. (2011). Influence of Atlantic sea surface temperatures on persistent drought in North America. *Climate Dynamics*, *37*(3–4), 569–586.

Frei, A., Kunkel, K. E., & Matonse, A. (2015). The seasonal nature of extreme hydrological events in the Northeastern United States. *Journal of Hydrometeorology*, *16*(5), 2065–2085.

Heim, R. R., Vose, R. S., Lawrimore, J. H., & Cook, E. R. (2007). Putting current North

America drought conditions into a multi-century perspective. Part 2: Using the blended product in operational drought monitoring. In *AGU Fall Meeting Abstracts*.

Ho, M., Lall, U., & Cook, E. R. (2018). How Wet and Dry Spells Evolve across the Conterminous United States Based on 555 Years of Paleoclimate Data. *Journal of Climate*, *31*(16), 6633–6647.

Jaeger, K. L., Olden, J. D., & Pelland, N. A. (2014). Climate change poised to threaten hydrologic connectivity and endemic fishes in dryland streams. *Proceedings of the National Academy of Sciences*, *111*(38), 13894–13899.

Kam, J., & Sheffield, J. (2016). Changes in the low flow regime over the eastern United States (1962–2011): variability, trends, and attributions. *Climatic Change*, *135*(3–4), 639–653.

Kaufman, L., & Rousseeuw, P. J. (2009). *Finding groups in data: an introduction to cluster analysis* (Vol. 344). John Wiley & Sons.

Kroll, C., Luz, J., Allen, B., & Vogel, R. M. (2004). Developing a watershed characteristics database to improve low streamflow prediction. *Journal of Hydrologic Engineering*, *9*(2), 116–125.

Kroll, C., & Vogel, R. (2000). *A National Assessment of Low-Streamflow Estimation Using a Physically Based Statistical Methodology*. https://cfpub.epa.gov/ncer_abstracts/index.cfm/fuseaction/display.highlight/abstract/82/repo rt/2000

Ladd, M., Viau, A. E., Way, R. G., Gajewski, K., & Sawada, M. C. (2018). Variations in

precipitation in North America during the past 2000 years. *The Holocene*, *28*(4), 667–675.

Leigh, C., & Datry, T. (2017). Drying as a primary hydrological determinant of biodiversity in river systems: A broad *scale analysis*. *Ecography*, *40*(4), 487–499.

Lins, H. F. (2012). *USGS hydro-climatic data network 2009 (HCDN-2009)*. US Geological Survey.

Martin, G. R., & Arihood, L. D. (2010). *Methods for estimating selected low-flow frequency statistics for unregulated streams in Kentucky*. US Geological Survey.

Martin, G. R., Fowler, K. K., & Arihood, L. D. (2016). *Estimating selected low-flow frequency statistics and harmonic-mean flows for ungaged, unregulated streams in Indiana*. US Geological Survey.

McCabe, G. J., Betancourt, J. L., Gray, S. T., Palecki, M. A., & Hidalgo, H. G. (2008). Associations of multi-decadal sea-surface temperature variability with US drought. *Quaternary International*, *188*(1), 31–40.

Menne, M. J., Williams Jr, C. N., & Vose, R. S. (2010). Long-term daily and monthly climate records from stations across the contiguous United States. *Website Http://Cdiac. Ornl. Gov/Epubs/Ndp/Ushcn/Access. Html*.

Najafi, E., Devineni, N., Khanbilvardi, R. M., & Kogan, F. (2018). Understanding the Changes in Global Crop Yields Through Changes in Climate and Technology. Earth's Future, 6(3), 410-427.

Najafi, E., Pal, I., & Khanbilvardi, R. M.(2018). Diagnosing extreme drought characteristics

24

across the globe. 42nd NOAA Annual Climate Diagnostics and Prediction Workshop, doi:10.7289/V5/CDPW-NWS-42nd-2018

Najafi, E., Pal, I., & Khanbilvardi, R. M.(2019). Climate drives variability and joint variability of global crop yields. Science of The Total Environment.

Newman, A. J., Clark, M. P., Sampson, K., Wood, A., Hay, L. E., Bock, A., … Arnold, J. R. (2015). Development of a large-sample watershed-scale hydrometeorological data set for the contiguous USA: data set characteristics and assessment of regional variability in hydrologic model performance. *Hydrology and Earth System Sciences*, *19*(1), 209.

Oglesby, R., Feng, S., Hu, Q., & Rowe, C. (2012). The role of the Atlantic Multidecadal Oscillation on medieval drought in North America: Synthesizing results from proxy data and climate models. *Global and Planetary Change*, *84*, 56–65.

Pournasiri Poshtiri, M., & Pal, I. (2014). Variability of low flow magnitudes in the Upper Colorado River Basin: identifying trends and relative role of large-scale climate dynamics. *Hydrology and Earth System Sciences Discussions*, *11*(7), 8779–8802.

Pournasiri Poshtiri, M., & Pal, I. (2016). Patterns of hydrological drought indicators in major US River basins. *Climatic Change*, *134*(4), 549–563.

Pournasiri Poshtiri, M., Towler, E., & Pal, I. (2016). Streamflow drought indicators across conterminous United States. Boulder, CO: Research Data Archive at the National Center for Atmospheric Research, Computational and Information Systems Laboratory. https://doi.org/10.5065/D6QR4V9X

Pournasiri Poshtiri, M., Towler, E., & Pal, I. (2017). *Streamflow Drought Indicators for the Conterminous United States*. https://doi.org/doi:10.5065/D65D8QJH

Pournasiri Poshtiri, M., Towler, E., & Pal, I. (2018). Characterizing and understanding the variability of streamflow drought indicators within the USA. *Hydrological Sciences Journal*, 1–13.

Reynolds, L. V, Shafroth, P. B., & Poff, N. L. (2015). Modeled intermittency risk for small streams in the Upper Colorado River Basin under climate change. *Journal of Hydrology*, *523*, 768–780.

Rossi, M. W., Whipple, K. X., & Vivoni, E. R. (2016). Precipitation and evapotranspiration controls on daily runoff variability in the contiguous United States and Puerto Rico. *Journal of Geophysical Research: Earth Surface*.

Sadri, S., Kam, J., & Sheffield, J. (2016). Nonstationarity of low flows and their timing in the eastern United States. *Hydrology and Earth System Sciences*, *20*(2), 633–649.

Smakhtin, V. U. (2001). Low flow hydrology: a review. *Journal of Hydrology*, *240*(3), 147–186.

Smith, T. M., Reynolds, R. W., Peterson, T. C., & Lawrimore, J. (2008). Improvements to NOAA's historical merged land–ocean surface temperature analysis (1880–2006). *Journal of Climate*, *21*(10), 2283–2296.

Tallaksen, L. M., Madsen, H., & Clausen, B. (1997). On the definition and modelling of streamflow drought duration and deficit volume. *Hydrological Sciences Journal*, *42*(1), 15–33.

Timilsena, J., Piechota, T., Tootle, G., & Singh, A. (2009). Associations of interdecadal/interannual climate variability and long-term colorado river basin streamflow. *Journal of Hydrology*, *365*(3), 289–301.

U.S. EPA. (2017). Definition and Characteristics of Low Flows from DFLOW. Retrieved from https://www.epa.gov/waterdata/definition-and-characteristics-low-flows-dflow

Van Loon, A. F. (2013). *On the propagation of drought: how climate and catchment characteristics influence hydrological drought development and recovery*.

Vander Vorste, R., Mermillod-Blondin, F., Hervant, F., Mons, R., Forcellini, M., & Datry, T. (2016). Increased depth to the water table during river drying decreases the resilience of Gammarus pulex and alters ecosystem function. *Ecohydrology*, *9*(7), 1177–1186.

Vidal, J. P., Martin, E., Franchistéguy, L., Habets, F., Soubeyroux, J.-M., Blanchard, M., & Baillon, M. (2010). Multilevel and multiscale drought reanalysis over France with the Safran-Isba-Modcou hydrometeorological suite. *Hydrology and Earth System Sciences Discussions*, *14*(3), 459–478.

Waples, R. S., Pess, G. R., & Beechie, T. (2008). Evolutionary history of Pacific salmon in dynamic environments. *Evolutionary Applications*, *1*(2), 189–206.

Wohl, E. (2017). The significance of small streams. *Frontiers of Earth Science*, 1–10.

Yevjevich, V. M. (1967). An objective approach to definitions and investigations of continental hydrologic droughts. *Hydrology Papers (Colorado State University); No. 23*.

Zelenhasić, E., & Salvai, A. (1987). A method of streamflow drought analysis. *Water Resources*
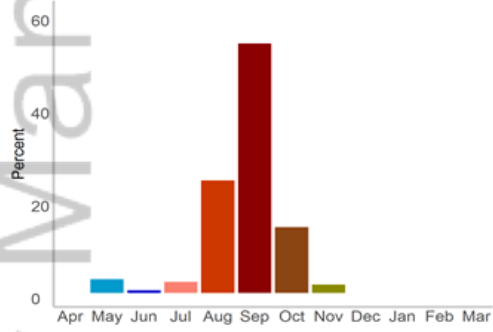
27

Research, *23*(1), 156–168.
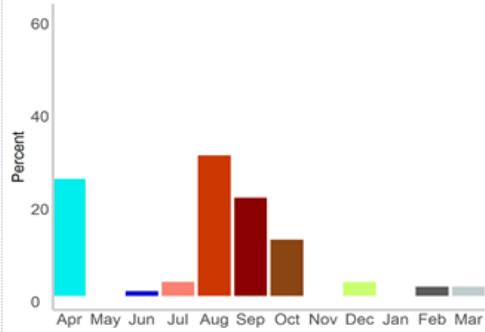
HYP_13422_F1.TIF

(a)

(b)
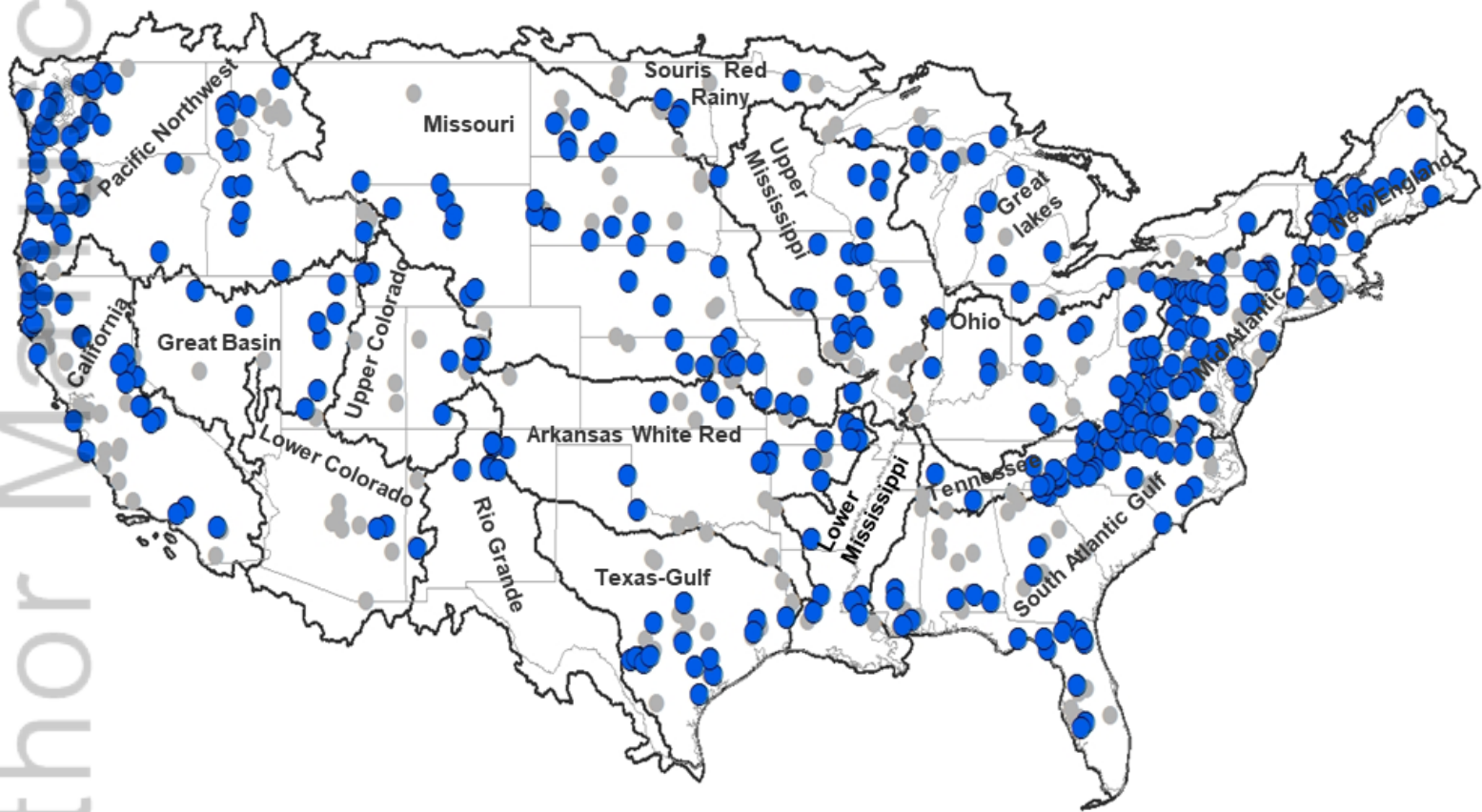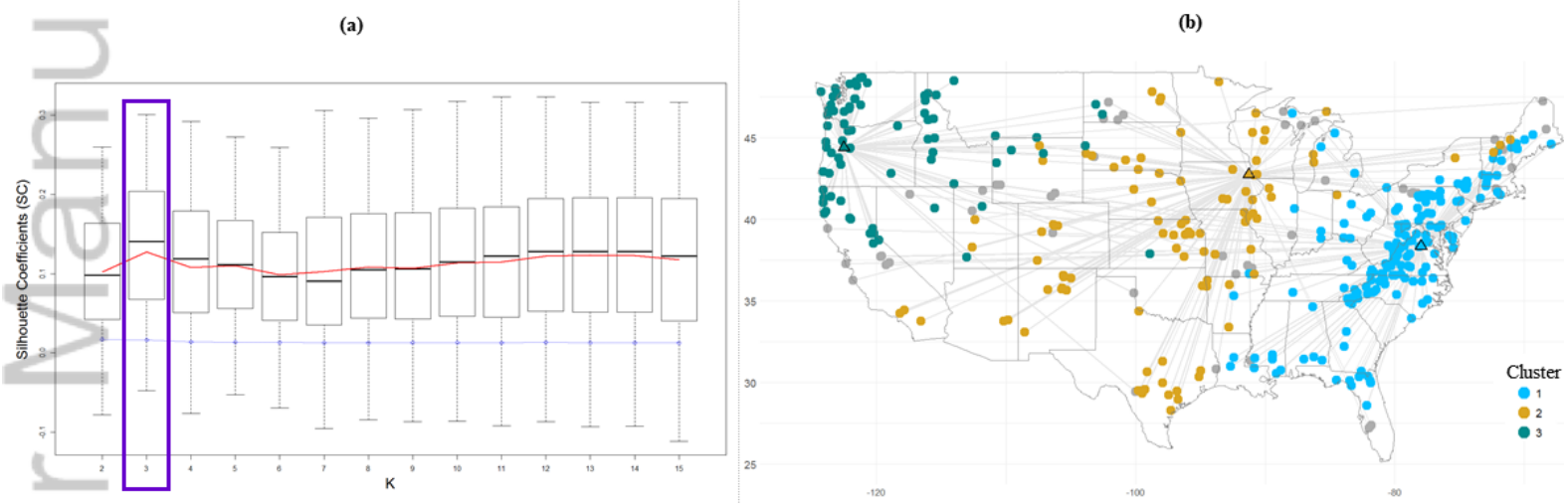
HYP_13422_F2.tif

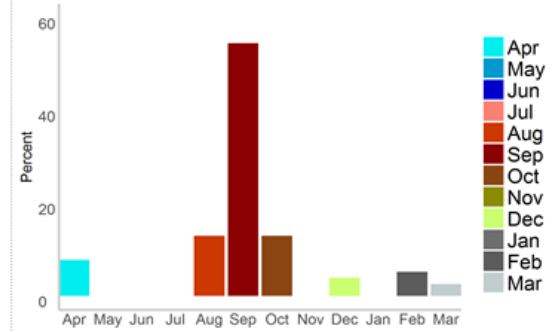(a) Cluster 1   (b) Cluster 2   (c) Cluster 3

HYP_13422_F3.tif

(a) PMDI   (b) P_{cpd} (c) T_{max} (d) T_{95}
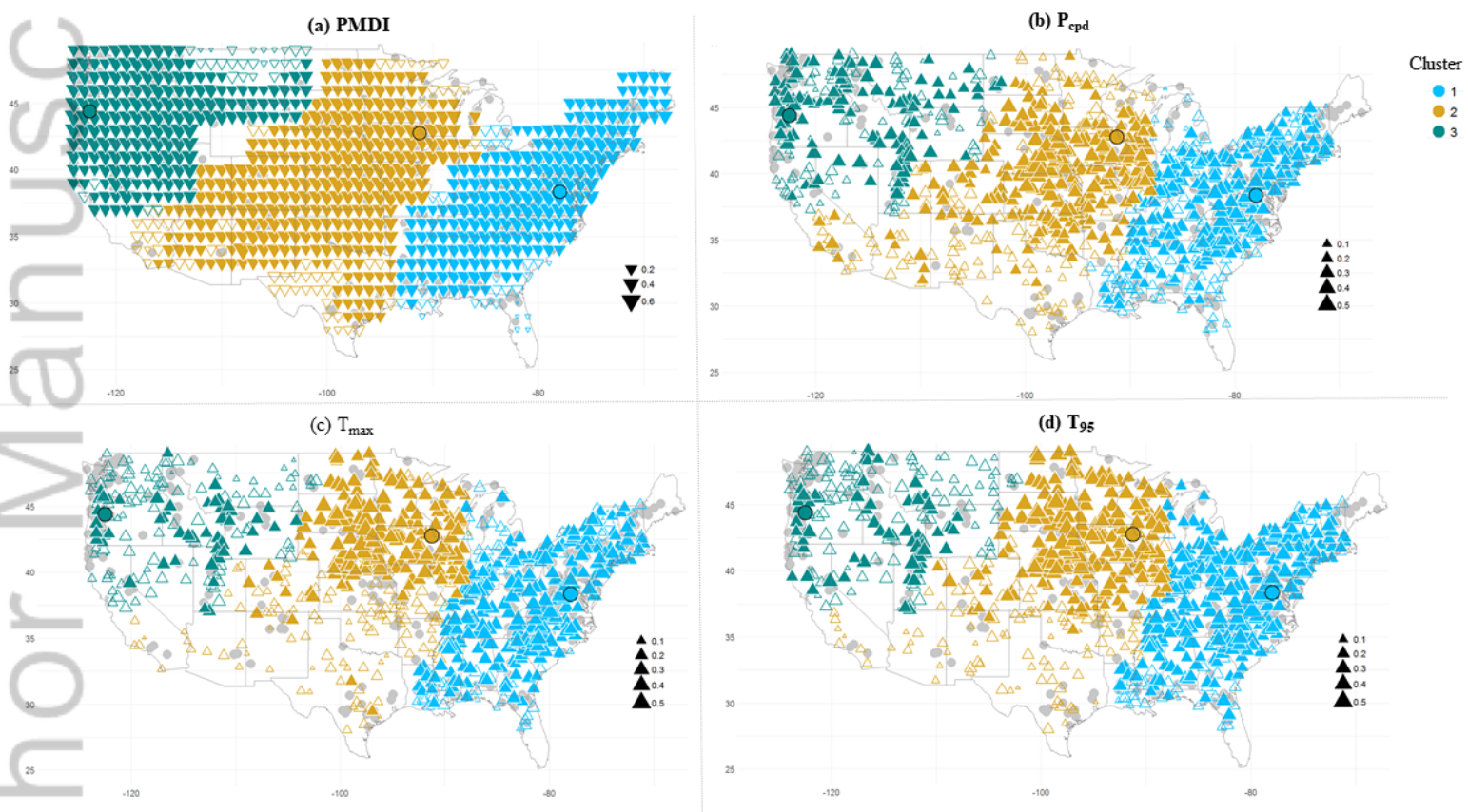
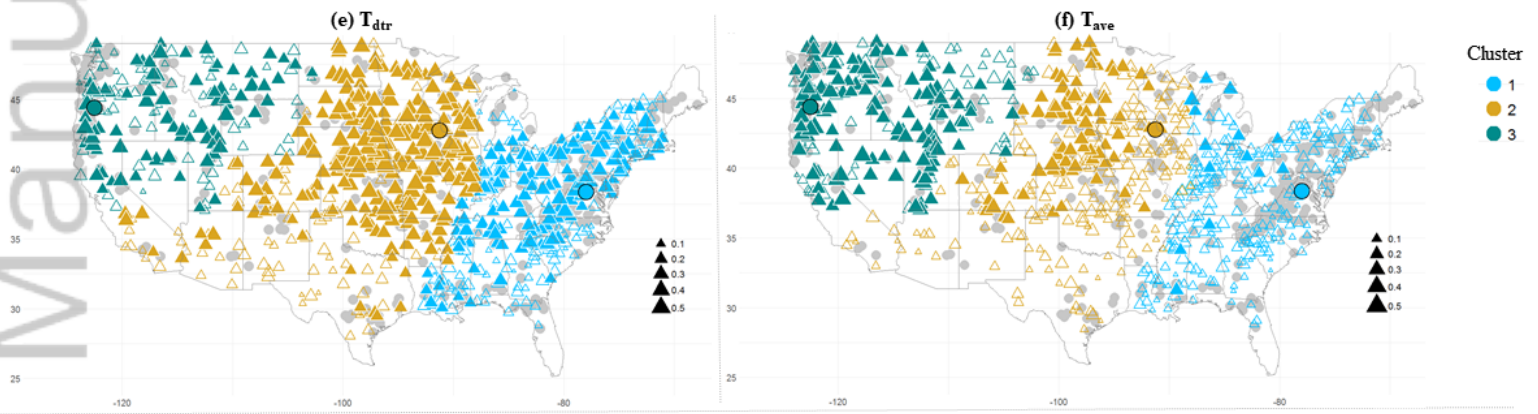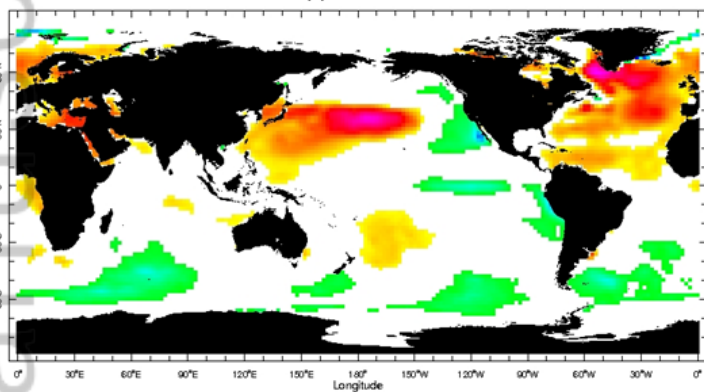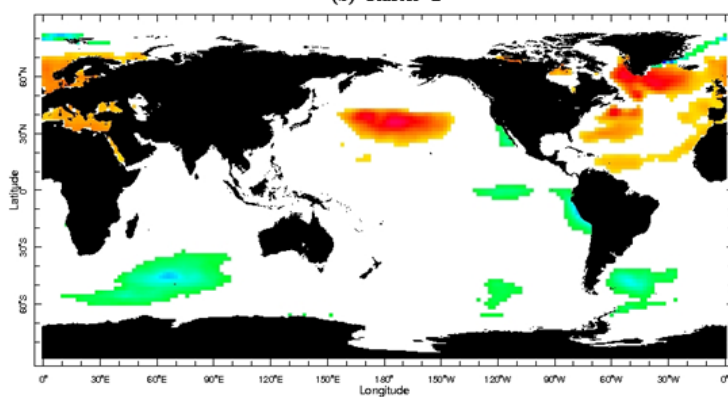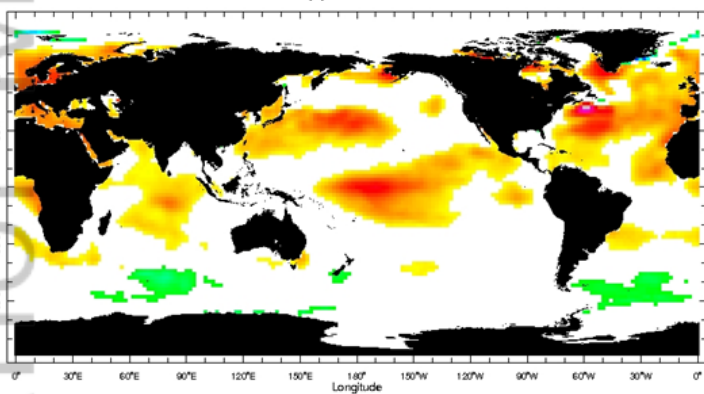HYP_13422_F4.1.TIF

HYP_13422_F4.2.TIF

(a) Cluster 1

(b) Cluster 2

(c) Cluster 3

HYP_13422_F5.tif